Supporting Information

Růžička et al. 10.1073/pnas.1005878107

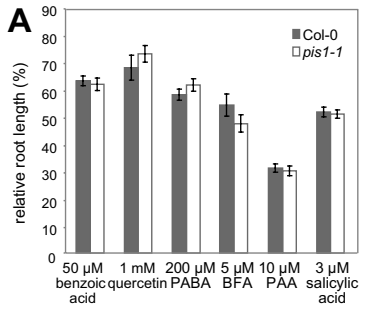

B

compound	hypersensitive *DR5::GFP* in *pis1-1*
2,4-D	10-50 nM
NPA	0.05-10 µM
IBA	0.5-5 µM

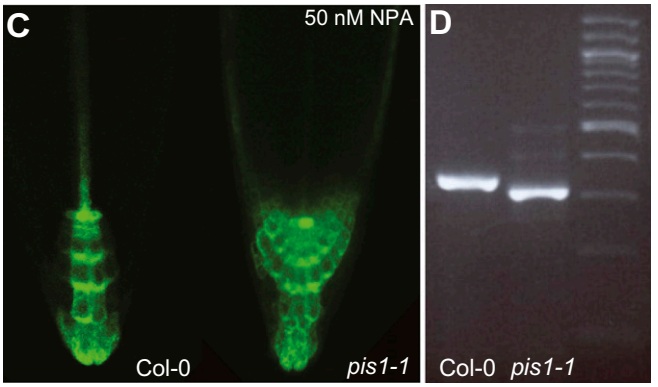

Fig. S1. Additional analyses of *pis1-1* allele of *ABCG37*. (*A*) Normal sensitivity of *abcg37 (pis1-1)* to various phytohormone-related substances and compounds structurally similar to auxins ($P > 0.05$ by ANOVA). (*B* and *C*) At a given detection limit, the *DR5rev::GFP* expression in *abcg37* (*pis1-1*) is more sensitive to the auxinic compounds (concentrations listed) as compared with the wild type (*B*). A representative image is shown also for NPA (*C*). (*D*) *pis1-1* mutation leads to an aberrant splicing of *ABCG37*. RT-PCR gel image shows the different length of the transcript in *pis1-1*. The altered splicing was confirmed by sequencing of the main transcript.

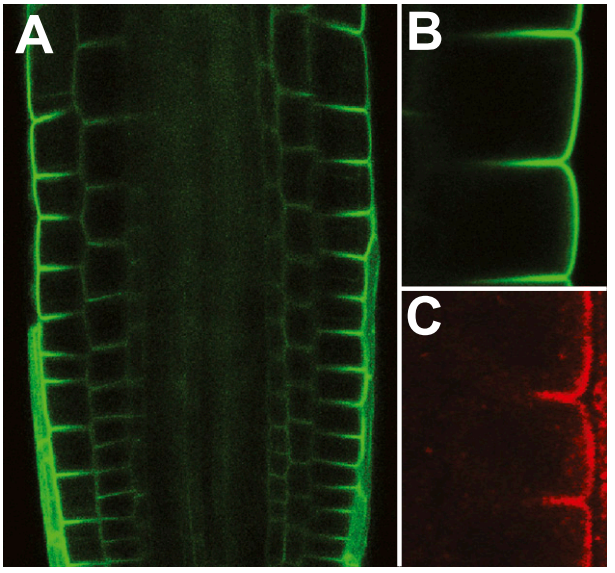

Fig. S2. ABCG37 is polarly localized at the outer side of root cells. (*A*) GFP-ABCG37 shows similar outer lateral localization pattern as observed by anti-ABCG37 immunolocalization. (*B*) Magnified view of epidermal cell files. (*C*) ABCG37 is normally localized in *abcg37/pdr9-1* gain-of-function mutant in anti-ABCG37 immunolocalization experiments.

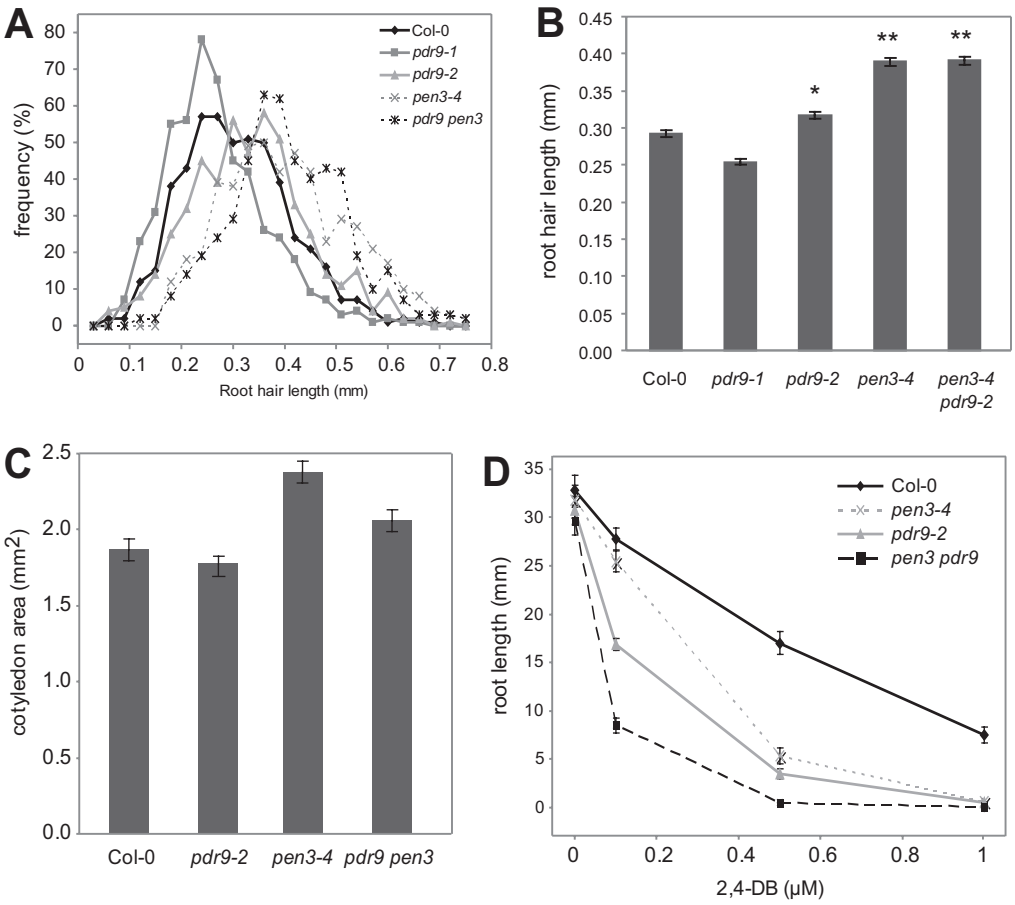

Fig. S3. Additional analyses of *abcg37* and *abcg36* phenotypes. (*A* and *B*) Loss-of-function (*pdr9-2* and *pen3-4*) or gain-of-function (*pdr9-1*) in *ABCG37* and *ABCG36* genes increases or decreases root hair frequency (*A*) (significantly different for each line, $P < 0.05$ by χ^2 test) and root hair length (*B*) (*, different from *pdr9-1*; **, different from Col-0; $P < 0.05$ by ANOVA). (*C*) Loss of *ABCG37* (*pdr9-2*) partially suppresses the increased cotyledon area conferred by loss of *ABCG36* (*pen3-4*) (Col-0 was different from *pen3-4*; *pdr9-2* was different from *pen3-4* and the double mutant; $P < 0.05$ by ANOVA). (*D*) Double *abcg36 abcg37* (*pen3-4 pdr9-2*) roots show enhanced sensitivity to 2,4-DB compared with either single mutant (single mutants were significantly different from the Col-0 control and the double mutant at 0.5 μM concentration point, $P < 0.05$ by ANOVA).

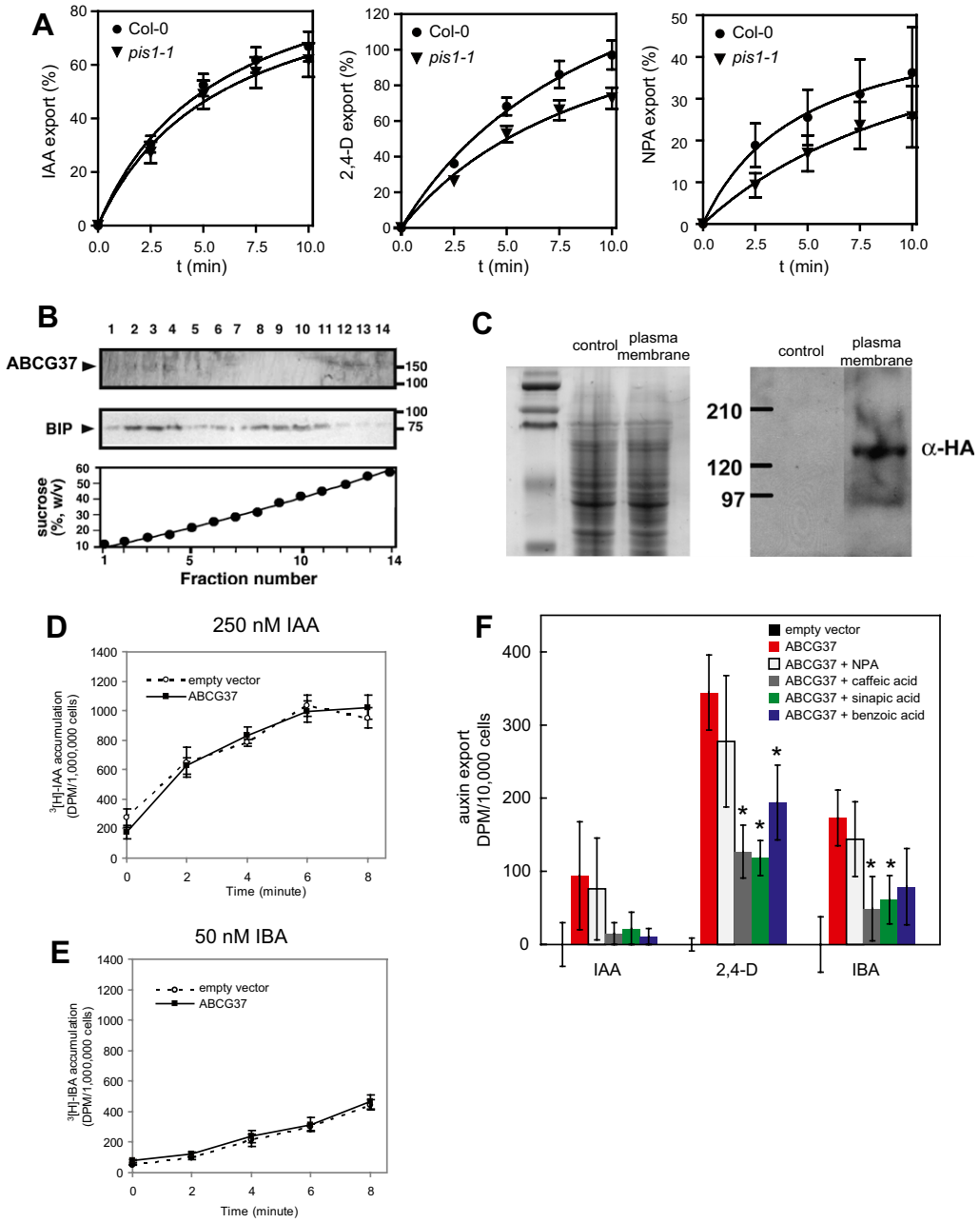

Fig. S4. Characterization of ABCG37, ABCB1, ABCB19, and PIN transport. (*A*) *abcg37* (*pis1-1*) leaf mesophyll protoplasts show significantly lower export of [^{3}H] 2,4-D and [^{3}H]NPA as compared with the wild type ($P < 0.05$ by ANOVA at 7.5-min time point), whereas [^{3}H]IAA export shows no significant difference between the two lines. (*B*) Immunoblotting of sucrose gradient fractions of yeast membrane extracts prepared from yeast expressing ABCG37 demonstrates that ABCG37 is enriched in comparable fractions as the marker BIP, indicating the ER localization of ABCG37 in yeast. (*C*) Two-phase partitioning demonstrates that *ABCG37* is localized on the plasma membrane in *S. pombe*. (*Left*) Coomassie blue-stained SDS/PAGE gel. (*Right*) Corresponding Western blot. (*D*) ABCG37 does not transport IAA, even at its saturating concentrations in *S. pombe* assays. (*E*) ABCG37 shows no significant transport capacity for lower amounts of IBA in *S. pombe* assays. (*F*) ABCG37 shows a broader specificity in HeLa cells assays (*, compound significantly competed with auxin tested; $P < 0.05$ by ANOVA).